Structural Modeling and Functional Analysis of the Essential Ribosomal Processing Protease Prp from *Staphylococcus aureus*

Erin A Wall[a,c], Adam L Johnson[a,d], Darrell L Peterson[b], Gail E Christie[a1]

Departments of [a]Microbiology and Immunology and [b]Biochemistry and Molecular Biology, Virginia Commonwealth University School of Medicine, Richmond VA 23298

[c]Current address: Laboratory of Molecular Biology, Center for Cancer Research, National Cancer Institute, Bethesda, MD 20892

[d]Current address: Department of Medicinal Chemistry, Virginia Commonwealth University School of Pharmacy, Richmond, VA 23298

[1]Communicating author

Supplementary Information

Table S1. Strains and Plasmids

Name	Description	Reference or source
***E. coli* strains**		
Stellar™	*E. coli* F^-, *endA1, supE44, thi-1, recA1, relA1, gyrA96, phoA, Φ80d lacZΔM15, Δ(lacZYA-argF)U169, Δ(mrr-hsdRMS-mcrBC), ΔmcrA,* λ^-	Clontech
BL21-CodonPlus™ (DE3)-RIL	*E. coli* B F^- *ompT hsdS*(r_8^- m_8^-) *dcm*$^+$ Tet^r *gal* λ(DE3) *endA* Hte [*argU ileY leuW* Cam^r]	Agilent Technologies
ScarabXpress ® T7 *lac*	Reduced genome T7 expression strain	Scarab Genomics
***S. aureus* strains**		
RN4220	Restriction-defective derivative of RN450	Kreiswirth *et al*., 1983
SA178RI	RN4220 derivative expressing T7 RNA polymerase from P_{spac}-*lacO*	D'Elia *et al*., 2006
ST256	SA178RI [pEW27] ; expresses L27 from T7*lac* promoter	This work
ST360	SA178RI L27::SpecR [pEW27] This strain is IPTG-dependent	This work
Plasmids		
pCN55	*E. coli/ S. aureus* shuttle vector containing *aad-9* $Spec^R$ cassette	Charpentier *et al*., 2004
pET21d(+)	*E. coli* T7 expression vector	Novagen
pET SUMO	TA cloning vector with SUMO tag	Invitrogen
pG164	*S. aureus* T7 expression vector	D'Elia *et al*., 2006
pHYRS52	His_6-tagged ULP1 protease expressed from T7*lac* promoter	Addgene
pMAD	*E. coli-S. aureus* shuttle vector for allelic exchange	Arnaud *et al*., 2004
pT104	P_{ars} expression vector for *S. aureus*	Liu *et al*., 2004
pRW	pET21d derivative for expression of proteins with an N-terminal His_6-SUMO tag	This work
pEW27	*S. aureus* L27 under T7 promoter, IPTG-inducible	Wall *et al*, 2015
pEW34	pRW derivative; His_6-SUMO-Prp wild-type	This work
pEW40	pRW derivative; His_6-SUMO-Prp C34S (TGT → AGT)	This work

pEW68	pMAD derivative; allelic exchange vector for replacement of L27 with $Spec^R$ cassette from pCN55	This work
pEW72	pT104 derivative; WT L27 expression in *S. aureus*	This work
pEW73	pT104 derivative; L27 Δ2-9 expression in *S. aureus*	This work
pEW74	pT104 derivative; L27 FF::AA expression in *S. aureus*	This work
pEW75	pT104 derivative; L27 Δ2-9 and L27 1-9 peptide expression in *S. aureus*	This work
pEW76	pG164 derivative; L27 Δ2-9 His_6 expression in *S. aureus* (for Edman degradation)	This work
pALJ5	pRW derivative; His_6-SUMO-Prp S38A (TCA → GCT)	This work
pALJ6	pRW derivative; His_6-SUMO-Prp D31A (GAT → GCA)	This work
pALJ7	pRW derivative; His_6-SUMO-Prp H22A (CAT → GCA)	This work
pALJ8	pRW derivative; His_6-SUMO-Prp G21A (GGC → GCA)	This work

References

Arnaud, M., Chastanet, A., and Debarbouille, M. (2004) New vector for efficient allelic replacement in naturally nontransformable, low-GC-content, gram-positive bacteria. *Appl Environ Microbiol* **70**: 6887-6891.

Charpentier, E., Anton, A.I., Barry, P., Alfonso, B., Fang, Yl, and Novick. R.P. (2004) Novel cassette=based shuttle vector system for gram-positive bacteria. *Appl Environ Microbiol* **70**: 6076-6085.

D'Elia, M.A., Pereira, M.P., Chung, Y.S., Zhao, W., Chau, A., Kenney, T.J., et al. (2006) Lesions in teichoic acid biosynthesis in *Staphylococcus aureus* lead to a lethal gain of function in the otherwise dispensable pathway. *J Bacteriol* **188**: 4183-4189.

Kreiswirth, B.N., Lofdahl, S., Betley, M.J., O'Reilly, M., Schlievert, P.M., Bergdoll, M.S., and Novick, R.P. (1983) The toxic shock syndrome exotoxin structural gene is not detectably transmitted by a prophage. *Nature* **305**: 709-712.

Liu, J., Dehbi, M., Moeck, G, Arhin, F, Bauda, P., Bergeron, D., et al. (2004) Antimicrobial drug discovery through bacteriophage genomics. *Nat.Biotechnol* **22**: 185-191.

Wall, E.A., Caufield, J.H., Lyons, C.E., Manning, K.A., Dokland, T., and Christie, G.E. (2015) Specific N-terminal cleavage of ribosomal protein L27 in *Staphylococcus aureus* and related bacteria. *Mol Microbiol* **95**: 258-269.

Table S2. Primers

Primers are organized based on the plasmids constructed, and templates are indicated. The annealing sequence for amplification is underlined and the 5' 15-16 bp homologous overhang required for the In-Fusion reaction is separated from the rest of the primer by an asterisk (*). Restriction sites used to linearize the plasmid prior to assembly are shown in bold in the sequence when they were reconstituted in the finished assembly or, in the case of pRW, for cleavage and ligation. Parentheses indicate a codon change for site-directed mutagenesis. Double asterisks (**) indicate that these primers were not used for PCR but were annealed to form a ds DNA fragment that was assembled during the In-Fusion reaction.

pEW34 *Template: RN4220*	
EAW101	AGA ACA GAT TGG AGG* C ATG ATT ACT GTT GAT ATT ACA GTT AAT GAT GAA GG
EAW102	GTG CGG CCG CAA GCT* TCA CTT ATA ATT TAA TCT AAT ATT CTC ATT ATA TTC TTC TTC AAT
pEW40 *Template: pEW35 (Wall et al. 2015)*	
EAW101	AGA ACA GAT TGG AGG* C ATG ATT ACT GTT GAT ATT ACA GTT AAT GAT GAA GG
EAW102	GTG CGG CCG CAA GCT* TCA CTT ATA ATT TAA TCT AAT ATT CTC ATT ATA TTC TTC TTC AAT
pEW68 *Templates: EAW 45+196 amplify L27 5' flank from RN4220, EAW197+198 amplify the aad9 SpecR cassette from pCN55 (Charpentier et al 2004), EAW199+48 amplify L27 3' flank from RN4220*	
EAW45	CGA TGC ATG **CCA TGG** *TAT ACA GGA GGT GCA AAG TAT GTT TGC TAT TAT TG
EAW196	CGG AAT GCA CCT CAC TTA TAA TTT AAT CTA ATA TTC TCA TTA TAT TC
EAW197	GTG AGG TGC ATT CCG * ATC GAA TCC CTT CGG AGC G
EAW198	CCG CGG TAA TAA ACT ATC GAA GGA AC
EAW199	AGT TTA TTA CCG CGG * GCA GTA GCT GAA TAA TTT TGT CTA GTT AAC ACC
EAW48	GGC GAT ATC **GGA TCC** *TTT ACC ACC GTC ACC GCC
pEW72 *Template: pEW27 (Wall et al, 2015)*	
EAW217	GTT GAT GAG G**GG ATC***C** ATG TTA AAA TTA AAC TTA CAA TTC TTC GCA TCT A
EAW218	GCT AAG CTT G**GT CGA*** **C** TTA TTC AGC TAC TGC ATA TAC AGA AAC TTG TTT TTT G
pEW73 *Template: RN4220*	

EAW223	GTT GAT GAG G**GG ATC*** **C** ATG GCA TCT AAA AAA GGG G
EAW218	GCT AAG CTT G**GT CGA*** **C** TTA TTC AGC TAC TGC ATA TAC AGA AAC TTG TTT TTT G
pEW74 *Template: pEW41 (Wall et al, 2015)*	
EAW224	GTT GAT GAG G**GG ATC*C** ATG TTA AAA TTA AAC TTA CAA GCA GC
EAW218	GCT AAG CTT G**GT CGA*** **C** TTA TTC AGC TAC TGC ATA TAC AGA AAC TTG TTT TTT G
pEW75	
EAW227**	TAA GTC GAC C**AA GCT*T** AGG AGG TGG ATC ATG TTA AAA TTA AAC TTA CAA TTC TTC TAA **A*AGC TT**A GCT AGC TAG
EAW228**	CTA GCT AGC T**AA GCT*T** TTA GAA GAA TTG TAA GTT TAA TTT TAA CAT GAT CCA CCT CCT **A*AGC TT**G GTC GAC TTA
pEW76 *Template: RN4220*	
EAW88	GAA AGG AGG T**GG ATC C** *ATG GCA TCT AAA AAA GGG GTA AGT TCT ACA AAA AAC G
EAW229	GCA GGA GCT C**GA ATT *C** TTA ATG ATG ATG ATG ATG ATG TTC AGC TAC TGC ATA TAC AGA AAC TTG TTT TTT G
pALJ7 *Template: RN4220*	
EAW101	AGA ACA GAT TGG AGG* C ATG ATT ACT GTT GAT ATT ACA GTT AAT GAT GAA GG
EAW185	GTC AGC (TGC) GCC ATC* CAT AAT AAC GTC TGT TAC TTT G
EAW186	GAT GGC (GCA) GCT GAC* CATG GTG AAT ATG GTC
EAW102	GTG CGG CCG CAA GCT* TCA CTT ATA ATT TAA TCT AAT ATT CTC ATT ATA TTC TTC TTC AAT
pALJ5 *Template: RN4220*	
EAW101	AGA ACA GAT TGG AGG* C ATG ATT ACT GTT GAT ATT ACA GTT AAT GAT GAA GG
EAW189	TAC AGC (AGC) AGC TCC* AGC ACA AAC GAT ATC ATG ACC
EAW190	GGA GCT (GCT) GCT GTA* TTG TTT GGT AGT GTT AAT GCG ATT ATA GG
EAW102	GTG CGG CCG CAA GCT* TCA CTT ATA ATT TAA TCT AAT ATT CTC ATT ATA TTC TTC TTC AAT
pALJ6 *Template: RN4220*	
EAW101	AGA ACA GAT TGG AGG* C ATG ATT ACT GTT GAT ATT ACA GTT AAT GAT GAA GG

EAW191	AAC GAT (TGC) ATG ACC* ATA TTC ACC ATG GTC AGC ATG
EAW192	GGT CAT (GCA) ATC GTT* TGT GCT GGA GCT TCA GC
EAW102	GTG CGG CCG CAA GCT* TCA CTT ATA ATT TAA TCT AAT ATT CTC ATT ATA TTC TTC TTC AAT
pALJ8 *Template: RN4220*	
EAW101	AGA ACA GAT TGG AGG* C ATG ATT ACT GTT GAT ATT ACA GTT AAT GAT GAA GG
EAW225	AGC ATG (TG)C ATC CAT* AAT AAC GTC TGT TAC TTT GCC TTC
EAW226	ATG GAT G(CA) CAT GCT* GAC CAT GGT GAA TAT GGT C
EAW102	GTG CGG CCG CAA GCT* TCA CTT ATA ATT TAA TCT AAT ATT CTC ATT ATA TTC TTC TTC AAT
pRW *Template: pET SUMO (Invitrogen)*	
SUF2	GG**C CAT GG**G CAG CAG CCA TCA TCA TC
SUR	CC**G GAT CC**G AGG CCT CCA ATC TGT TCT CTG TGA GCC

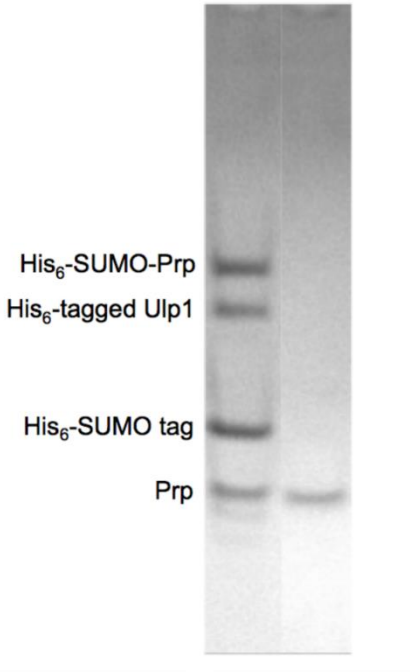

Figure S1. SDS-PAGE of Prp pre- and post-purification.

The left lane of this composite gel shows the products present in the His6-SUMO-Prp:His6-tagged Ulp1 cleavage reaction after initial elution from a Ni-NTA column, before re-purification by nickel affinity chromatography. The right lane shows purified, tagless Prp that was eluted during the second nickel affinity chromatography purification step.

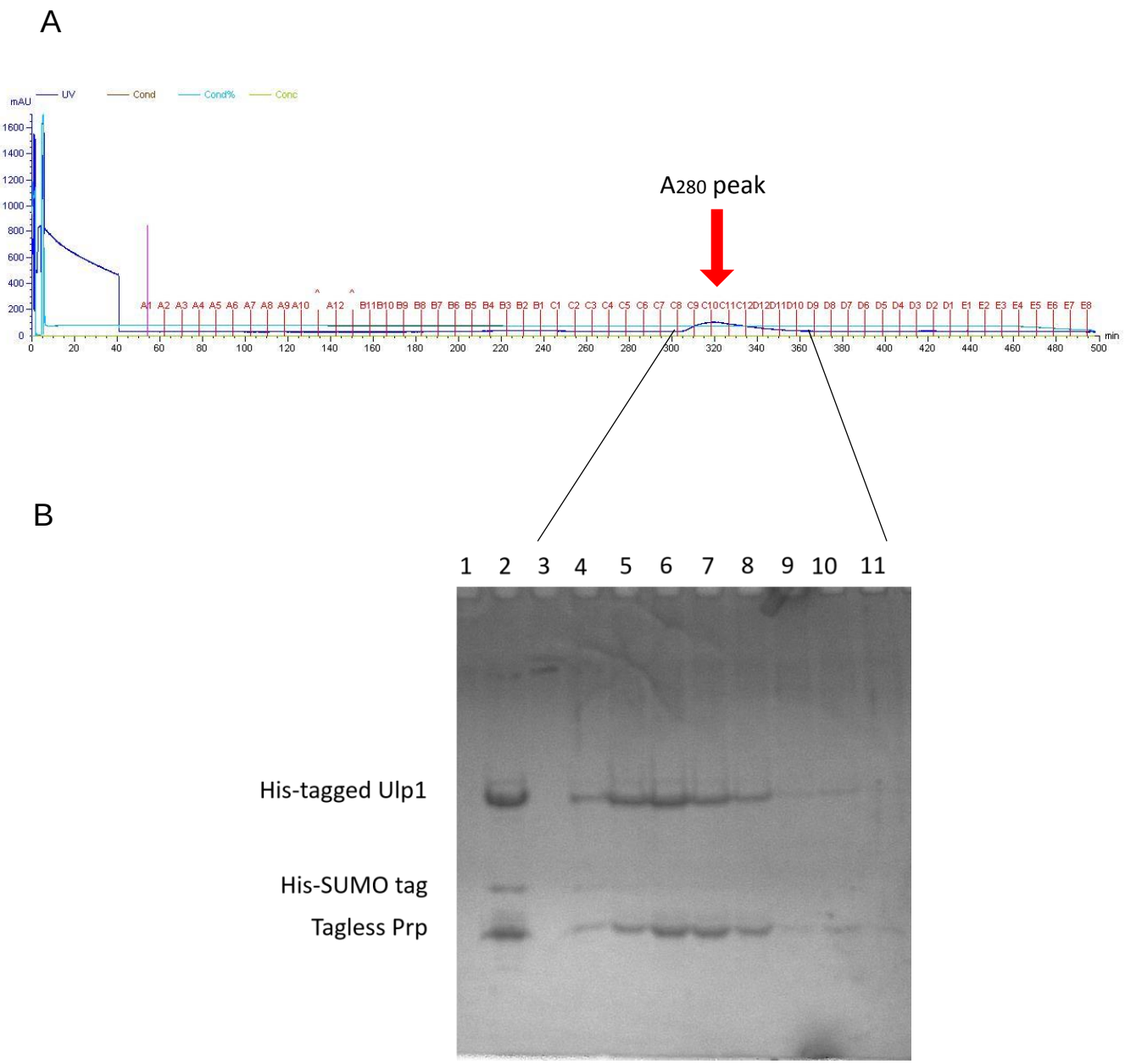

Figure S2. Size exclusion chromatography demonstrates that Prp is a dimer in solution

A. A concentrated sample of the cleavage reaction containing His-SUMO-Prp and His-tagged Ulp1 was purified via FPLC on a P10 size-exclusion column (MWCO 20,000). One peak eluted over fractions C8-D10. These fractions were analyzed by SDS-PAGE and showed that tag-less Prp (MW 11,691.79) had co-eluted with His-tagged Ulp1 (MW 27,394.05), indicating that Prp is a dimer with an approximate MW of 23,383.

B. SDS-PAGE gel showing tagless Prp (MW 11,691.79) co-eluted from a P10 size-exclusion column with His-tagged Ulp1 (MW 27,394.05), indicating Prp is a dimer (MW ~23,383). Lane 1-blank, 2-His-SUMO-Prp cleavage reaction, 3-blank, 4-C8, 5-C9, 6-C10, 7-C11, 8-C12, 9-D12, 10-D11, 11-D10

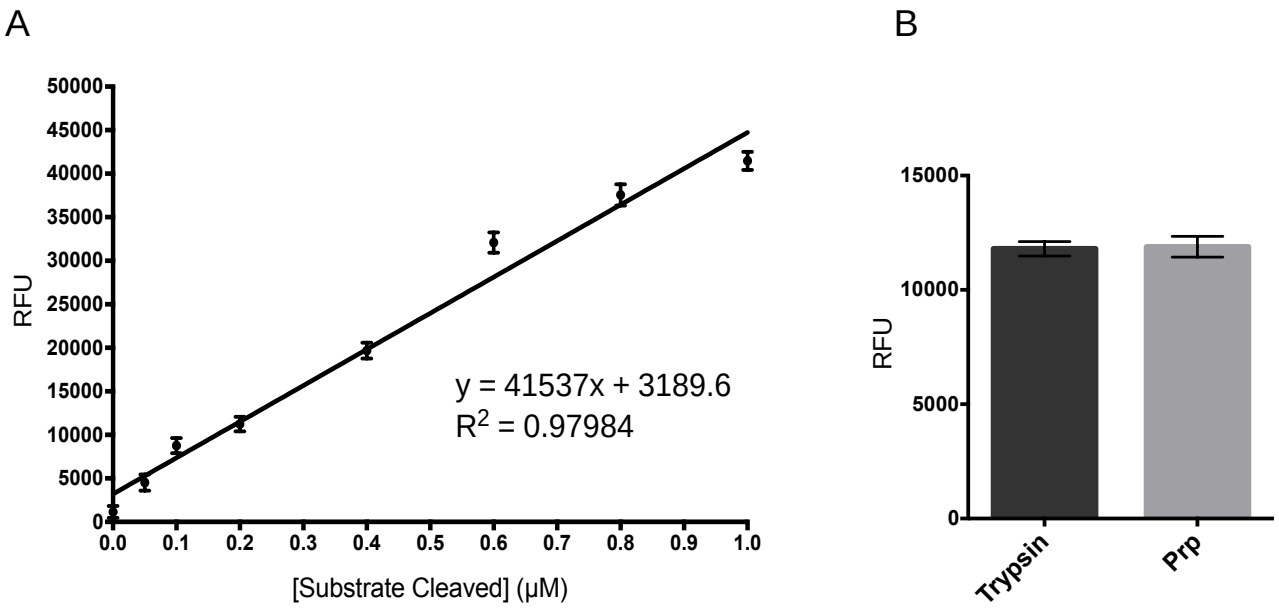

Figure S3. Conversion of fluorescence to substrate concentration.

A. Standard curve generated by cleaving varying amounts of fluorogenic peptide using trypsin. The fluorogenic peptide contains three lysine sites that trypsin can cleave. The equation of the standard curve was used to convert the raw RFU values from Prp assays to concentrations of substrate cleaved.

B. Cleavage of 2 μM fluorogenic substrate with 10μg of trypsin or Prp. The absolute RFU values from four completed reactions were averaged. These results indicate that both reactions proceeded to the same extent of completion. The RFU axis is different from that in A because the gain of the spectrophotometer was adjusted downward.

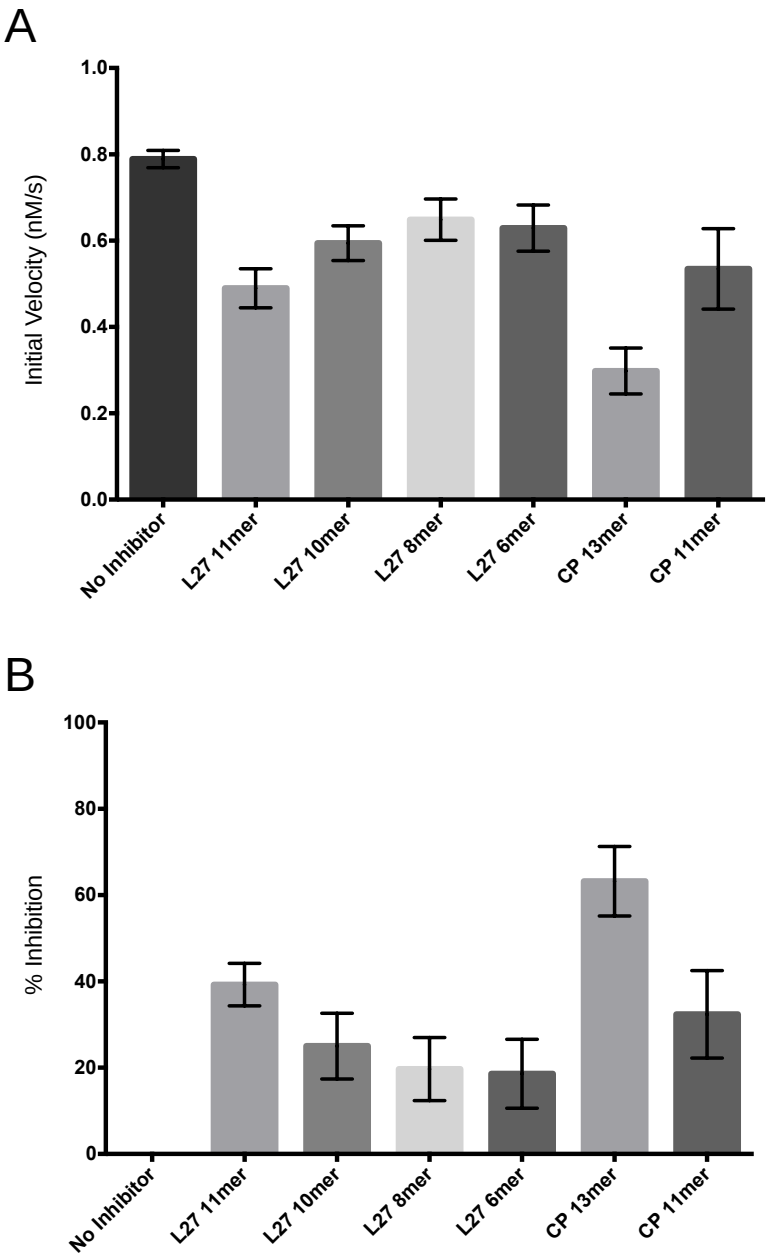

Figure S4. Effects of competitive peptides on Prp activity

A. The average initial velocity for reactions containing 29.3 nM Prp and 0.8 μM of each peptide inhibitor. Sequences of peptides are given in Table 1. n ≥ 3; bars indicate 1 standard deviation.

B. Percent activity for each peptide assayed in A. Values were calculated relative to the no-inhibitor control and converted to average percent inhibition.

Figure S5A. Ribbon model of Prp dimer. Catalytic residues and the modeled flexible loop between them are depicted. The His and Cys are arranged in a pro-catalytic conformation and ionized. His 22 is always on a flexible loop due to preceding Gly 21.

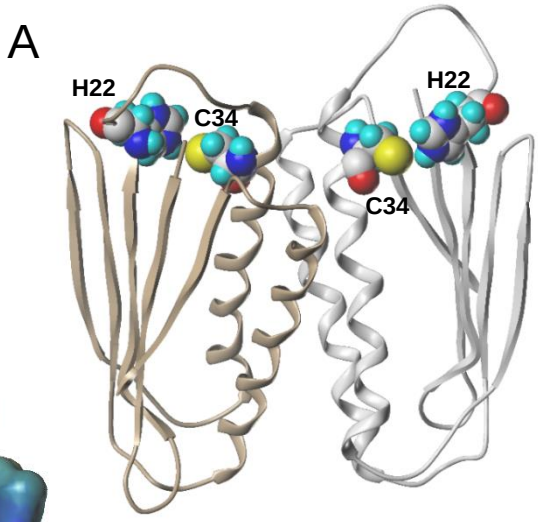

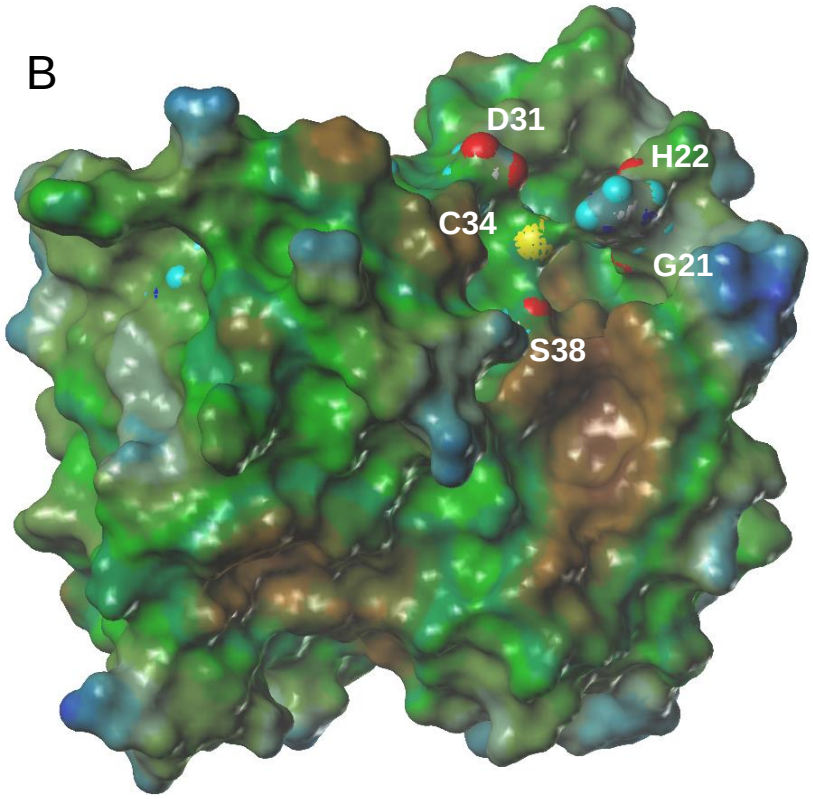

Figure S5B. Surface hydrophobicity map of Prp dimer. Conserved residues around the active site are labeled. Hydrophobic regions are depicted in brown and hydrophilic regions in blue, with green representing a median value. A large hydrophobic patch appears below the catalytic center, presenting a likely binding region for hydrophobic residues in the substrate. The hydrophobic patch on the bottom of the other chain could be where residues at the N-terminus of the cleavage motif bind.

Figure S5C. Surface hydrophobicity map of Prp dimer with docked peptide. Conserved residues around the active site are labeled. Docked peptide Ac-NLQFFAS-Am is depicted in white surface and atomic color convention. Here the sidechain of extremely conserved P3 Gln in the substrate protrudes into solvent, apparently making no contact with the enzyme. This paired with the lack of substrate binding by the extremely conserved Asp 31 sidechain makes it seem even more likely that the flexible loop somehow folds over the substrate during catalysis, perhaps associating these two residues.